

# Separation and cleaning of *Leymus chinensis* seed threshing material based on gas-solid coupling

Zongyu Ma<sup>1</sup>, Qihao Wan<sup>2\*</sup>, Weiwei Liu<sup>1</sup>, Yingzhong Zhang<sup>1</sup>, Ku Bu<sup>2</sup>, Wenliang Du<sup>3</sup>

(1. School of Mechanical Engineering, Dalian University of Technology, Dalian 116024, China;

2. Institute of Grassland Research, Chinese Academy of Agricultural Sciences, Hohhot 010010, China;

3. College of Mechanical and Electrical Engineering, Inner Mongolia Agricultural University, Hohhot 010018, China)

**Abstract:** The aim of this study was to improve the cleaning performance of the *Leymus chinensis* seed threshing material separation and cleaning device, and to clarify the movement law and characteristics of the *Leymus chinensis* seed threshing material during the cleaning process. A numerical simulation of the separation and cleaning process of *Leymus chinensis* seed threshing material was performed using the computational fluid dynamics discrete element approach. According to the streamline distribution of the gas-solid coupling, the movement of *Leymus chinensis* seeds during the cleaning process was examined. Additionally, the average speed and quantity of *Leymus chinensis* seed threshing material in different separation and cleaning zones were studied over time. Meanwhile, the distribution principle of the threshing material was obtained, and a verification test of the under-sieve distribution was conducted. The test results showed that the numerical simulation was consistent with the distribution trend of the under-sieve. The cleaning performance verification test showed that the impurity content and the loss rate of the separation and cleaning device were 27.3% and 3.3%, where the test results, compared with those of the numerical simulation, showed a reduction of 1.5% and 0.8%, respectively. It is feasible to apply the theory and method of gas-solid coupling to simulate the separation and cleaning process of *Leymus chinensis* seeds.

**Keywords:** cleaning performance, gas-solid coupling, *Leymus chinensis* seeds, numerical simulation, separation and cleaning

**DOI:** [10.25165/j.ijabe.20231605.8140](https://doi.org/10.25165/j.ijabe.20231605.8140)

**Citation:** Ma Z Y, Wan Q H, Liu W W, Zhang Y Z, Bu K, Du W L. Separation and cleaning of *Leymus chinensis* seed threshing material based on gas-solid coupling. *Int J Agric & Biol Eng*, 2023; 16(5): 283–290.

## 1 Introduction

China is a large grassland territory with a natural grassland area of approximately 400 million hm<sup>2</sup> and a usable grassland area of approximately 220 million hm<sup>2</sup>. These grassland areas are mainly distributed in the northeast and western regions of Inner Mongolia and other northwestern regions, as well as in western Sichuan. Exploiting the advantages of such a usable grassland area is crucial for promoting the economic development and ecological protection of the country. *Leymus chinensis* (*Leymus chinensis* (Trin.) Tzvel.) is a plant belonging to the family of Gramineae and *Leymus*. It is an important forage grass occurring naturally in pastures in eastern Inner Mongolia and the western northeast, and it has a strong tolerance to the environment<sup>[1]</sup>. In addition to serving as forage, *Leymus chinensis* has developed rhizomes and a remarkable ability to maintain and strengthen soil fertility. Thus, the plant is an excellent water and soil conservation plant. In addition, the stems of *Leymus chinensis* are a raw material for papermaking<sup>[2]</sup>. These advantages necessitate strengthening the research on *Leymus*

*chinensis* seed breeding and cultivation of fine varieties to increase the seed propagation, expand the planting area, and increase the grass seeds harvest to upgrade forage yield. However, *Leymus chinensis* seed harvesting machinery is still immature, as it faces problems such as a large harvest loss and low seed cleaning rate. These problems have hindered the development of the *Leymus chinensis* industry<sup>[3]</sup>.

Currently, the main methods of harvesting grass seeds, such as *Leymus chinensis*, locally and abroad involve direct harvesting with a combined harvester for grains, direct harvesting with a dedicated grass seed harvester without cutting the stems, and the use of windrowers for picking and harvesting. Various machine harvesting methods have been studied<sup>[4,5]</sup>. The full-feed combine harvesting method uses a combine harvester for cutting, threshing, grass seed winnowing, cleaning, collecting, and performing other operations simultaneously. It presents several advantages such as high work efficiency and reduced labor intensity and is suitable for large-scale production. This is the current mainstream harvest method<sup>[6,7]</sup>. A full-feed combine harvester is used to harvest the *Leymus chinensis* seeds. This is because the harvester can cut the stalks of the *Leymus chinensis* while the seeds are harvested and use the rake and baler to collect and bundle the straws, respectively, through its “pipeline.” The technique of operation can improve work efficiency, save cost, and meet the requirements of agricultural modernization. Therefore, the study of harvesting *Leymus chinensis* seeds using the full-feeding combined harvesting method is crucial for promoting the development of gramineous forage seed harvesting<sup>[8]</sup>.

Separation and cleaning is a crop cleaning method commonly used by combine harvesters. The performance of the separation and cleaning device determines the operating quality of the entire machine. Thus, to improve the performance of the separation and

**Received date:** 2023-01-08 **Accepted date:** 2023-06-10

**Biographies:** **Zongyu Ma**, PhD candidate, research interest: modern machine design and optimization, Email: [mazongyu108@163.com](mailto:mazongyu108@163.com); **Weiwei Liu**, PhD, Associate Professor, research interest: sustainable design and manufacturing, Email: [liuww@dlut.edu.cn](mailto:liuww@dlut.edu.cn); **Yingzhong Zhang**, PhD, Professor, research interest: sustainable design and manufacturing, Email: [zhangyz@dlut.edu.cn](mailto:zhangyz@dlut.edu.cn); **Ku Bu**, Researcher, research interest: design and intelligence of grassland machinery, Email: [buku0471@163.com](mailto:buku0471@163.com); **Wenliang Du**, Professor, research interest: modern machine design and optimization, Email: [duwl58@163.com](mailto:duwl58@163.com).

**\*Corresponding author:** **Qihao Wan**, PhD, Assistant Researcher, research interest: design and intelligence of grassland machinery. Institute of Grassland Research Chinese Academy of Agricultural Sciences, Hohhot 010010, China. Tel: +86-15184721626, Email: [wanjihao204@sina.com](mailto:wanjihao204@sina.com).

cleaning device for the seeds of *Leymus chinensis*, researchers need to study the operating principles of the device. Owing to the complexity of the cleaning process, it is difficult to study the movement laws and material characteristics during the cleaning process through traditional experimental methods. The gas-solid coupling theory has been widely used in the material cleaning and separation research<sup>[9-11]</sup>. Feng et al.<sup>[12]</sup> used computational fluid dynamics and the discrete element method (CFD-DEM) to investigate the motion of particles at different stages of screening and the effect of airflow velocity above the sieve on the dispersion degree of particles, which provided a theoretical basis for improving the cleaning performance. Li et al.<sup>[13]</sup> conducted CFD-DEM simulations of the movement of rice in an air-and-screen cleaning shoe. The effect of inlet airflow velocity is studied and analyzed in terms of grains and short straws' longitudinal velocity and vertical height, and cleaning loss. It showed that numerical simulation of material motion on vibrating screen of air-and-screen cleaning device based on CFD-DEM is feasible. Gao et al.<sup>[14]</sup> designed a sieve with three-dimensional translational motion based on a cylindrical cam to improve the working efficiency of the cleaning device for maize mixture with a large feeding mass and to realize rapid dispersion of the maize grains on the sieve.. CFD-DEM was used to investigate the motion of materials on the three-dimensional translational vibrating sieve, and this research provides a reference for the design of multidimensional motion sieve for large feed volume grain cleaning. Ding et al.<sup>[15]</sup> investigated the working

mechanism of the existing single-duct cleaning device using CFD-DEM in order to optimize the paddy single-duct cleaning device to meet the requirements of large feeding capacity and evaluated the cleaning performance in terms of the movement pattern of the threshing output in the cleaning shoe. While most of the above studies were conducted on crops such as corn, wheat and rice; unfortunately, the cleaning process of forage seeds such as *Leymus chinensis* is more complicated. Therefore, according to the gas-solid coupling theory<sup>[10,11,16]</sup>, This research used the CFD-DEM approach to numerically simulate the separation and cleaning process of *Leymus chinensis* seeds threshing material in the device, study the movement laws and characteristics of *Leymus chinensis* seed threshing materials, and determine the dynamic of the speed and quantity of threshing materials in different zones. The results of this study are expected to provide a research and development reference for the *Leymus chinensis* seed separation and cleaning device and combine harvester.

## 2 Structure and working principle of the wind screen cleaning device

### 2.1 Structural composition

The separation and cleaning system used in the test included automatic feeding, cleaning, receiving, and transmission devices, along with the frequency conversion control system. The structure is illustrated in Figure 1.

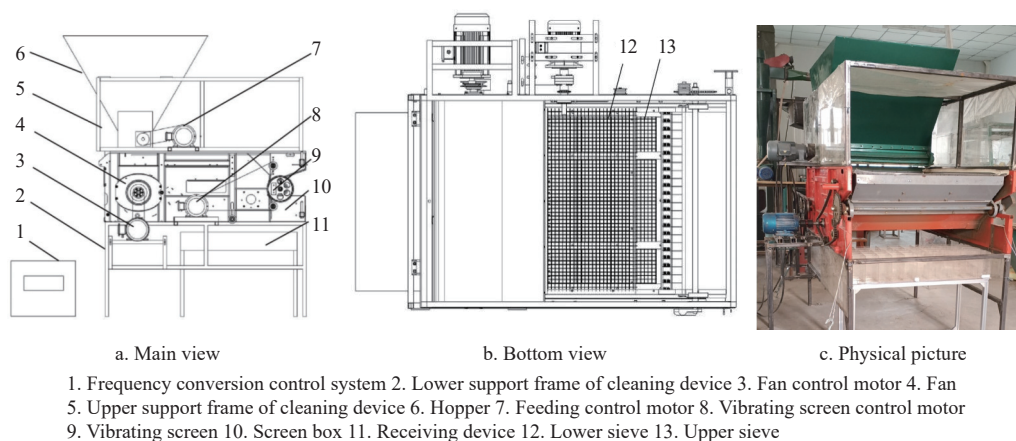


Figure 1 Structural diagram of separation and cleaning device for the threshing material of *Leymus chinensis* seeds

To be as consistent as possible with the combine harvester used for field harvesting, the screen box of the separation and cleaning device has the same model and size as that of the field full-feed combine harvester. The operating parameters, such as the vibration frequency of the vibrating screen, rotation frequency of the fan, and rotation frequency of the feeding device, were controlled and adjusted by the frequency converter. The screens of the upper sieve and the lower sieve could be disassembled to be replaced with others of different forms and sizes. Fifty-five small sampling boxes were installed on the receiving device to analyze the distribution pattern of the under-sieve. The main technical parameters of the separation and cleaning device are listed in Table 1.

### 2.2 Working process

During the working process, the feeding amount of the *Leymus chinensis* seed threshing material in the hopper is controlled by the feeding-rate frequency conversion controller. *Leymus chinensis* seeds fall on the shaking plate of the vibrating screen, and the frequency conversion controller of the vibrating screen adjusts the

vibration frequency to evenly transport the *Leymus chinensis* seeds forward. When the *Leymus chinensis* seed threshing material just touches the sieve surface, a part of the light impurities is blown out of the outlet directly under the action of the fan, which is also

Table 1 Main technical parameters of *Leymus chinensis* seed extractive air sieve cleaning device

Technical parameter	Numerical value
Overall dimensions (length×width×height)/mm	2024×1548×2370
Overall quality/kg	550
Working machine power/kW	3.85
Structure type	Fixed
Upper sieve type (length×width)/mm(Long hole or square hole woven screen, replaceable)	996×1090
Lower sieve type (length×width) /mm(Long hole or square hole woven screen, replaceable)	996 × 530
Rated speed of vibrating screen / r·min <sup>-1</sup>	1400
Rated fan speed / r·min <sup>-1</sup>	2840
Rated speed of feeding device/r·min <sup>-1</sup>	1730

controlled by the fan frequency controller to set the wind speed. The *Leymus chinensis* seeds and short stalks then fall on the upper sieve through the shaking plate, some of the stalks are directly discharged from the upper sieve to the discharge opening, and most of the stalks and seeds fall onto the lower sieve. The material on the lower sieve contains most of the stalks and part of the *Leymus chinensis* seeds, which fall to the re-extraction device. After the shutdown, the materials in the re-separation device are returned to the hopper for recycling cleaning. The material under the sieve contains a small part of the stem and most of the *Leymus chinensis* seeds, and they fall into the receiving device where they are collected. During the screening process of the vibrating screen, the wind continually blows out some light impurities, seed bran, short stalks with low suspension speed, and weed seeds.

### 3 CFD-DEM coupling theory

The fluid phase continuity equation and momentum equation can be expressed as follows<sup>[17]</sup>:

$$\frac{\partial(\varepsilon_f \rho_f)}{\partial t} + \nabla \cdot (\varepsilon_f \rho_f \mu_f) = 0 \quad (1)$$

$$\frac{\partial(\varepsilon_f \rho_f \mu_f)}{\partial t} + \nabla \cdot (\varepsilon_f \rho_f \mu_f \mu_f) = -\nabla p + \nabla \cdot (\mu_f \varepsilon_f \nabla \mu_f) - \varepsilon_f \rho_f g - S \quad (2)$$

where,  $\rho_f$  is fluid density, kg/m<sup>3</sup>;  $t$  is time, s;  $\mu_f$  is fluid flow rate, m/s;  $\varepsilon_f$  is fluid volume fraction;  $p$  is fluid pressure, Pa;  $\mu_f$  is fluid viscosity, Pa·s;  $S$  is momentum sink, N/m<sup>3</sup>.  $\nabla$  is Hamilton operator;  $g$  is gravity, 9.8 m/s<sup>2</sup>.

The coupling between the two phases is then achieved through the calculation of the momentum sink of the drag force that arises due to the relatively velocity between the phases. Therefore, the momentum sink  $S$  is calculated by following equation<sup>[18]</sup>

$$S = \frac{1}{\Delta V} \sum_{i=1}^n F_{D,i} \quad (3)$$

where,  $\Delta V = \Delta x \Delta y \Delta z$ ,  $\Delta x$ ,  $\Delta y$  and  $\Delta z$  are the length of the control body in  $x$ ,  $y$ , and  $z$  directions respectively, m;  $F_{D,i}$  is fluid viscous resistance of particle  $i$ , N.

$$F_{D,i} = 0.5 C_D \rho_f A_p (u_f - u_p) \cdot |u_f - u_p| \varepsilon_f^{-(\chi+1)} \quad (4)$$

The porosity correction function  $\varepsilon_f^{-(\chi+1)}$  in Equation (4) represents the influence of the packing concentration of grains on the drag force. The expression for the term  $\chi$  is

$$\chi = 3.7 - 0.65 \exp \left[ \frac{-(1.5 - \lg Re)^2}{2} \right] \quad (5)$$

$$C_D = \left( 0.63 + \frac{4.8}{Re^{0.5}} \right)^2 \quad (6)$$

$$Re = \frac{\varepsilon_f \rho_f d_p |u_f - u_p|}{\mu_f} \quad (7)$$

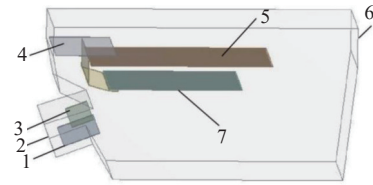
where,  $\chi$  is the coefficient;  $C_D$  is fluid resistance coefficient;  $d_p$  is the particle diameter;  $u_p$  is the particle velocity;  $Re$  is Reynolds number.

## 4 Model establishment and parameter setting

### 4.1 Model building and meshing

The length, width, and height of the screen box were 1500 mm, 1080 mm, and 600 mm, respectively. Because the structure is symmetrical in the width direction, the established model was simplified to speed up the simulation; the width was 500 mm, and the remaining dimensions were consistent with the actual size. The

*Leymus chinensis* seeds separation cleaning device model mainly comprised an inlet, an upper sieve, a lower sieve, a shaking plate, an upwind separation board, a downwind separation board, and an outlet, as illustrated in Figure 2. The upper sieve was a woven sieve with 16 mm×6 mm openings, and the lower sieve was a woven sieve with 16 mm×4 mm openings. The separation and cleaning device was modeled using SolidWorks 2018 and imported into Workbench 18.0 for solving; Finally, the meshing using the Mesh module. The mesh quality significantly influences the calculation accuracy and precision of the results<sup>[19]</sup>. The obtained model of the screening device was highly complicated. In order to improve the adaptability of the mesh to the geometry, an unstructured tetrahedral mesh is used<sup>[20,21]</sup>. The average quality of grids is 0.739 and the number of grids of the model is 78 831, as shown in Figure 3.

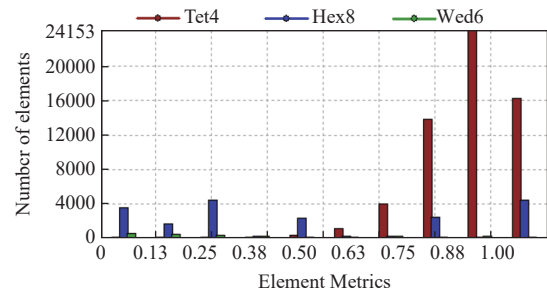


1. Downwind separation board 2. Inlet 3. Upwind separation board  
4. Shaking plate 5. Upper sieve 6. Outlet 7. Lower sieve

Figure 2 Model of windscreen cleaning device



a. Divided grid



b. Mesh quality

Figure 3 Mesh division

### 4.2 Material model and parameter settings

Short stalks are the most difficult to clean out of *Leymus chinensis* seeds threshing material. Therefore, a discrete elemental model of *Leymus chinensis* seeds and short stalks was established. The triaxial dimensions of the *Leymus chinensis* seeds were 7.17 mm length, 1.10 mm width, and 0.80 mm thickness. Fourteen spheres were used to fit the shape of the *Leymus chinensis* seeds accurately. The triaxial dimensions of the short stalks were 36.1 mm in length and 1.5 mm in diameter, and 27 spheres were used to fit the model. The models are shown in Figure 4.

To accurately and effectively complete the numerical simulation of the vibration cleaning of *Leymus chinensis* seeds, setting the material parameters in the discrete element model, material parameters of the vibrating screen, and contact and

collision parameters between them<sup>[20,22]</sup>. The parameter settings are listed in Table 2, and the contact collision parameters are listed in Table 3.

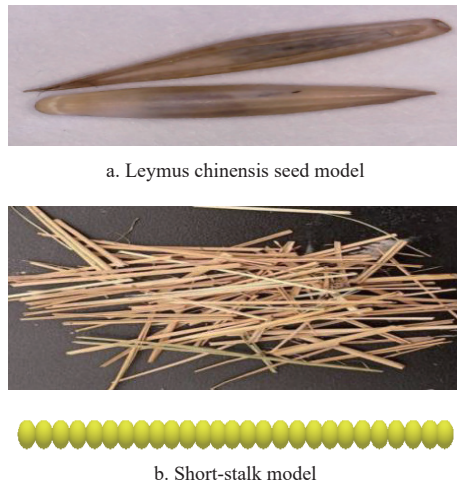


Figure 4 Material model construction

Table 2 Material parameter settings

Category	Density/kg·m <sup>-3</sup>	Shear modulus/MPa	Poisson's ratio
Leymus chinensis seeds	286	2.1	0.25
Short stalk	356	1.0	0.4
Vibrating screen	7850	807	0.3

Table 3 Contact and collision parameter settings

Category	Coefficient of restitution	Coefficient of static friction	Rolling friction coefficient
Seed-seed	0.44	0.80	0.25
Seed-short stalk	0.30	0.50	0.17
Seed-vibrating screen	0.45	0.30	0.12
Short stalk-short stalk	0.22	0.50	0.15
Short stalk-vibrating screen	0.30	0.36	0.10

According to the actual harvesting operation, the feed rate of the separation and cleaning device was set to 0.08 kg/s, and the number of Leymus chinensis seeds and stalks was set according to its ratio of grain to straw.

### 4.3 Coupling parameter settings of the model

The boundary conditions in Fluent18.0 state were set as follows. The inlet was the velocity inlet, wind speed was 5 m/s, outlet was the pressure outlet, rest was set as the wall surface, and material was stainless steel. According to the actual cleaning device, the upper air distribution plate angle was set to 35° in the model, the angle of the lower air distribution plate was 30°, standard *k-ε* turbulence model was selected in the calculation process, and SIMPLEC algorithm was used to calculate the flow field. In EDEM2018, the Hertz-Mindlin non-slip contact model was selected as the contact model, and the soft ball model was selected as the contact method<sup>[23]</sup>. CFD-DEM coupling allows Lagrangian and Eulerian models. The Lagrangian model only considers the momentum exchange between the fluid and solid phases, whereas the Eulerian model considers the momentum exchange between the fluid and solid phases as well as the pair of solid particles. The influence of the fluid was considered important; therefore, the Eulerian model was used for simulation<sup>[24]</sup>. Time step matching in the CFD-DEM was a crucial step. The time step of EDEM is typically smaller than that of CFD. If the two are adjusted to an integer multiple relationship, the coupling module automatically matches. In the process of coupling simulation, the time step of EDEM was determined by the Rayleigh time-step, in which the time step of EDEM was 20% of that of Rayleigh, and the time-step of Fluent was 100 times that of EDEM<sup>[25]</sup>. Here, the time step in Fluent was set to 3e-4, time step in EDEM was set to 3e-6, and total simulation time was 3 s.

## 5 Simulation process and result analysis

### 5.1 Movement law of threshing material in the process of separation and cleaning

Figure 5 illustrates the simulation process of the separation and cleaning of Leymus chinensis threshing material at various moments when the wind speed was 5 m/s, amplitude was 30 mm, frequency was 5 Hz, and vibration direction angle was 35°. The streamline diagram shows that when  $t=0.03$  s, the threshing material of Leymus chinensis seeds began to fall onto the shaking plate. When  $t=0.15$  s, under the shaking action of the shaking plate, the material began to fall onto the sieve surface, and a small amount of Leymus chinensis seeds passed through the upper sieve. At  $t=0.27$  s, some Leymus chinensis seeds and short stalks passed through the upper sieve, and some small impurities were blown out of the outlet.

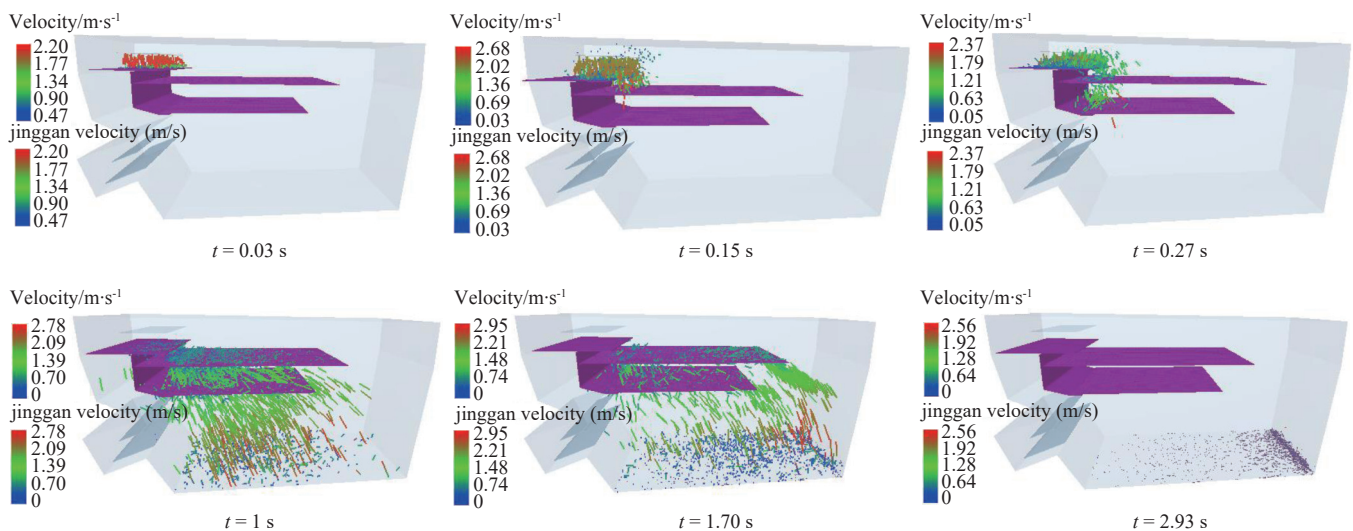


Figure 5 CFD-DEM coupling numerical simulation process of Leymus chinensis seed threshing material

When  $t=1$  s, the pellet factory was cut, and the stalks were discharged from the upper sieve under the action of the vibrating screen and fan, and most of the *Leymus chinensis* seeds fell into the receiving device through the lower sieve. When  $t=1.7$  s, the material on the shaking plate had fallen on the sieve surface, and most of the *Leymus chinensis* seeds were screened. At this time, the stalks reached the middle and rear ends of the upper sieve, where the wind speed was higher. Large stalks were accelerated for separation. When  $t=2.93$  s, the screening process was completed. The material distribution under the screen shows that the material was divided into three parts. The small particles at the front were *Leymus chinensis* seeds, which were collected by the receiving device; the middle was also made of *Leymus chinensis* seeds in a mixture with short stalks, and this part fell to the re-separation position and finally returned to the hopper for re-sieving; the last part was entirely made of the stalk, which was directly separated from the waste discharge port.

**5.2 Changes in *Leymus chinensis* seed threshing material rate**

To analyze the screening process better, five statistical areas were set in the cleaning device model, as shown in Figure 6. The first one was located above the shaking plate and used to count the falling quantity and speed of materials; the second one was located above the upper sieve and used to count the quantity and movement speed of materials; and the third one was located above the lower sieve and used to count the number of materials here. The fourth was located under the lower sieve, and according to the receiving box of the actual receiving device, it was set up as 55 small squares in five horizontal rows and 11 vertical rows, which were used to count the amount of material retained under the sieve. The fifth zone was located at the discharge opening and used to count the loss of *Leymus chinensis* seeds.

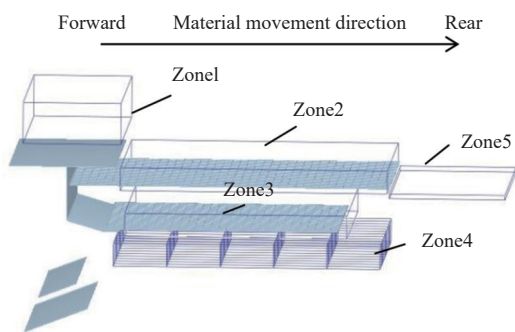
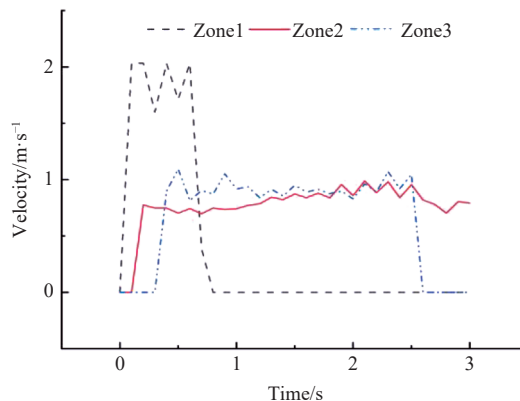


Figure 6 Statistics area settings

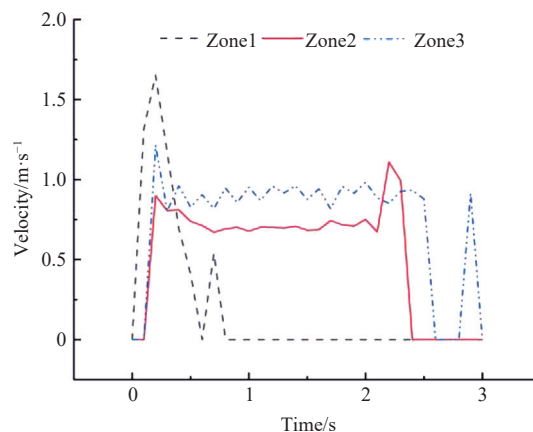
Figure 7 depicts the curve of the average velocity of the *Leymus chinensis* seed threshing material in different zones with time. The figure shows that all the *Leymus chinensis* seeds fell onto the shaking plate in approximately 1 s. At this time, under the influence of wind speed, the falling speed of *Leymus chinensis* seeds was slower than that of the stalk and more stable than that of the stalk. The average speed of the short stalks in zones 2 and 3 was the same. The average speed of *Leymus chinensis* seeds in zone 3 was significantly higher than the average speed of zone 2. This is because the *Leymus chinensis* seeds in zone 3 had no short stalks. The blocked material was separated faster.

Figure 8 illustrates the change in the average velocity of the *Leymus chinensis* seed threshing material over time in area 2. The figure shows that the moving speed of the *Leymus chinensis* seed threshing material was relatively stable, and the average speed of the *Leymus chinensis* seed and stalk was 0.8 m/s. In the early stage, the movement speed of *Leymus chinensis* seeds was slightly higher

than the movement speed of the stalks, and the opposite was true in the later stage. This is because the seeds of the *Leymus chinensis* had been screened after 1.17 s, and the stalks continued to move backward under the action of the vibrating screen and the fan.



a. Speed change in different short-stalk areas



b. Speed change in *Leymus chinensis* seeds in different regions

Figure 7 Variation curve of average speed in different zones of *Leymus chinensis* seed threshing material with time

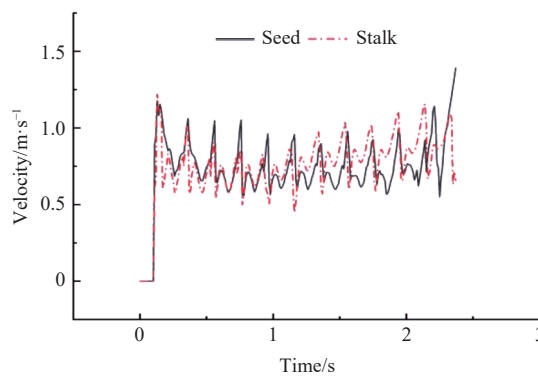
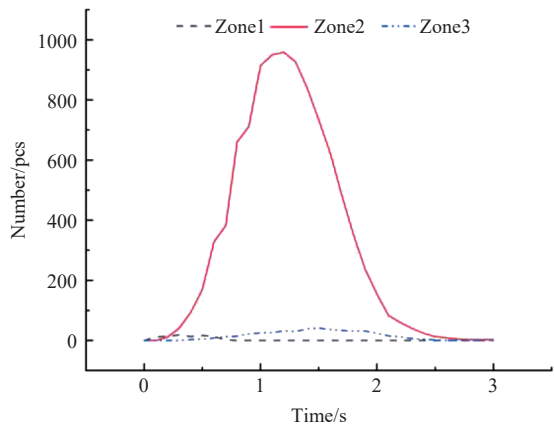


Figure 8 Change in the moving speed of the objects on the sieve over time

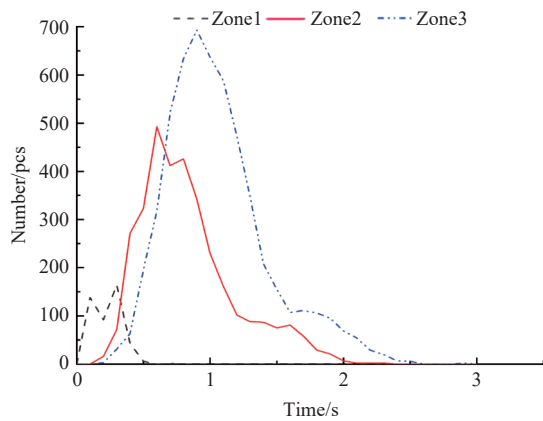
**5.3 Changes in the quantity of threshing materials for *Leymus chinensis* seeds**

Figure 9 illustrates the variation in the quantity of *Leymus chinensis* seeds in different separation and cleaning zones over time. As shown in Figure 9a, most of the short stalks were located in area 2, reaching the maximum value at 1.3 s. This zone represents the upper screen of the separation and cleaning device, and most of the short stalks were sieved from the upper sieve. As shown in Figure 9b, the number of *Leymus chinensis* seeds gradually increased from zone 1 to 3 over time and tended to zero after 2.5 s. Zone 3 was the lower screen of the air sieve cleaning device. As the screening

process progressed, most of the *Leymus chinensis* seeds fell onto the lower sieve, and almost all of them passed through the sieve after 2.5 s.



a. Variations in the number of short stalks in different areas



b. Changes in the number of *Leymus chinensis* seeds in different regions

Figure 9 Number of *Leymus chinensis* seed threshing material in different zones versus time

Figure 10 illustrates the change in the number of *Leymus chinensis* seeds through the sieve in zone 4 over time. The figure shows that the seeds of *Leymus chinensis* first increased and then decreased over time. At 0.22 s, the *Leymus chinensis* seeds started to pass through the sieve. When the 1 s blanking was completed, the screening process was stabilized, and the number of *Leymus chinensis* seeds through the sieve reached the maximum value. At 2.5 s, the screening process was completed, and the *Leymus chinensis* seeds were also completed through the screening. Twelve *Leymus chinensis* seeds were lost in zone 5.

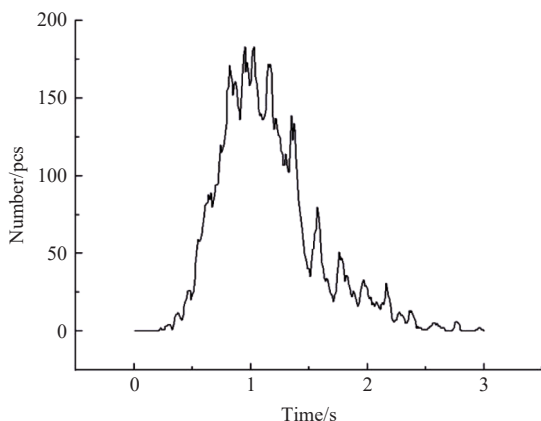
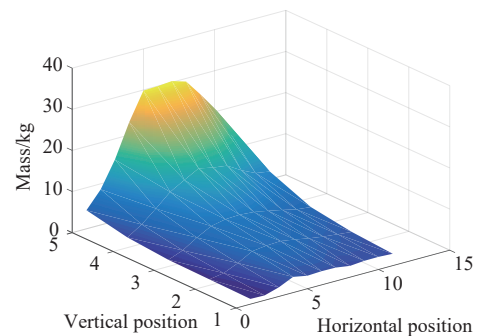


Figure 10 Changes in the quantity of *Leymus chinensis* seeds from the sieve over time

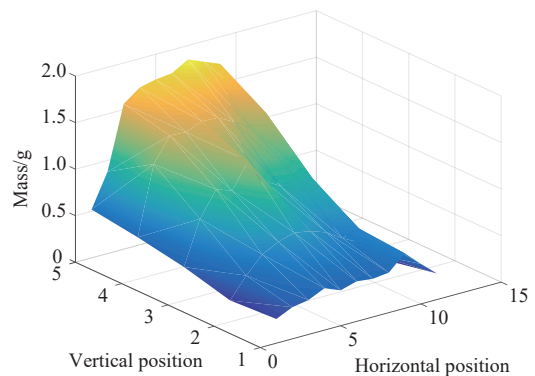
## 6 Experimental verification

### 6.1 Comparison of material distribution under the screen

To verify the accuracy of the numerical simulation results, on the built-up separation and cleaning device, a receiving device composed of 55 small square boxes was used to analyze the distribution of the under-sieve and compare it with the under-sieve in zone 4 in the numerical simulation. The distributions were compared, and the results are presented in Figure 11. The figure shows that the distribution patterns of the under-sieve in the actual test and the coupled simulation were the same, the under-sieve mass gradually increased from the front to the back in the direction of material movement, and the under-sieve mass in the middle position was greater than that on both sides. This is because under the action of the vibrating screen and wind, the under-the-screen materials move backward as a whole, and the wind speed increases near the rear end; therefore, most of the materials are distributed at the rear end. This phenomenon also verifies the reliability of the numerical simulation results. The actual receiving results are presented in Figure 12.



a. Distribution of the actual test sieve



b. Numerical simulation of the distribution of under-sieves

Figure 11 Comparison of the distribution of under-sieve materials between the numerical simulation and the test



Figure 12 Actual receiving result

### 6.2 Cleaning performance test

Based on the previous simulated experimental study, performance tests were conducted on the constructed *Leymus chinensis* seeds threshing material separation and cleaning device. A

detailed experimental study of the *Leymus chinensis* seeds threshing material separation and cleaning device performance was carried out in literature [26]. The four main factors selected for analysis that have a significant effect on the separation and cleaning performance are vibrating screen speed, fan speed, feed rate, and screen hole size. In the experimental results of the literature [26], the effect of vibrating screen speed on the cleaning performance is more complicated, lower or higher speed will affect the rate of impurities, with the increase of the vibrating screen speed, the rate of impurities shows a trend of first decreasing and then increasing, and the loss rate has been showing an increasing trend. The loss rate tended to increase with the increase of fan speed and rose sharply after reaching 1050 r/min, which indicated that the wind speed after 1050 r/min exceeded the suspension speed of sheep grass seeds, resulting in the sheep grass seeds being blown out of the discharge port without penetrating the sieve. The rate of impurity was decreasing and then increasing with the increase of feeding volume, and the rate of impurity was the lowest at the feeding volume of 0.02 kg/s. The loss rate was increasing with the increase of feeding volume.

In December 2020, conducted a performance test on a separation and cleaning device (Figure 13). The raw materials used in the test were threshing materials collected from a field full-fed combine harvester shaker plate. The *Leymus chinensis* seeds had a moisture content of 17.5%, ratio of grain to straw of 1:51.4, cleaning device vibrating screen speed of 275 r/min, fan speed of 985 r/min, and feed rate of 0.08 kg/s. The impurity and loss rates were used to test the test indicators. After the test was averaged three times, the impurity rate was 27.3%, and the loss rate was 3.3%. The cleaning effect of *Leymus chinensis* seeds was better, as shown in Figure 12. This was compared with the numerical simulation of the impurity rate (28.8%) and loss rate (4.1%), and the test results were lower only by 1.5% and 0.8%, respectively. In the previous study, Dai et al.<sup>[11]</sup> performed a numerical simulation of the flax threshing material separation cleaning process using CFD-DEM. Verification test results showed that the cleaning rate of separating cleaning device for flax threshing material was 92.66% with 1.58% of total separation loss. Compared with simulation results, the test results were 1.34% and 0.93% lower, showing that it is feasible to apply the gas-solid coupling theory and method to simulate the separating and cleaning operation of flax threshing material. The experimental results of this study were basically consistent with the simulation results, which also further verified the correctness of the simulation results of the separation and cleaning process of *Leymus chinensis* seed based on the CFD-DEM gas-solid coupling theory.



Figure 13 Work site and cleaning effect

## 7 Conclusions

1) According to the analysis of the working process of the *Leymus chinensis* seed separation and cleaning device, the CFD-DEM gas-solid coupling equation was established; the separation and cleaning device model and the *Leymus chinensis* seed threshing material model were established according to EDEM, and the fluid calculation domain was established using Fluent.

2) Numerical simulation of the movement process of the *Leymus chinensis* seed threshing material in the separation and cleaning device was conducted, and the migration pattern and movement characteristics of the *Leymus chinensis* seed threshing material during the cleaning process were obtained. Based on the streamline distribution of gas-solid coupling, the pattern of movement of *Leymus chinensis* seed threshing materials with time was investigated, and the average velocity and quantity of *Leymus chinensis* seed threshing material in different separation and cleaning zones were studied over time.

3) According to the comparison between the distribution of the under-sieve and that of the actual test, it was found that the distribution trend of the under-sieve from the experiment and the numerical simulation was consistent; the impurity rate and loss rate were used as the test indicators, and the cleaning performance test was conducted to obtain the impurity. The seed cleaning effect of *Leymus chinensis* was 27.3%, and the loss rate was 3.3%. Compared with the numerical simulation results, the experimental results were lower by 1.5% and 0.8%, respectively, and they were consistent with the simulation results. The results show that it is feasible to use the CFD-DEM gas-solid coupling theory as a method to simulate the separation and cleaning process of *Leymus chinensis* seed threshing material.

## Acknowledgements

The authors acknowledge that this work was financially supported by the Science and Technology Major Special Projects of Inner Mongolia Autonomous Region (Grant No. 2020ZD0002); Key Research and Achievements Transformation Plan Project of Inner Mongolia Autonomous Region (Grant No. 2022YFHH0053); the Inner Mongolia Autonomous Region Natural Science Foundation (Grant No. 2023MS03013).

## [References]

- [1] He X Q, Wang Y R, Hu X W, Baskin C C, Baskin J M, Lv Y Y. Seed dormancy and dormancy-breaking methods in *Leymus chinensis* (Trin.) Tzvel. (Poaceae). *Grass and Forage Science*, 2016; 71(4): 641–648.
- [2] Ren X H, Wang J, Ma X F. High-yielding cultivation and efficient utilization of *Leymus chinensis*. *Journal of Animal Science and Veterinary Medicine*, 2018; 37(2): 81–82, 84. (in Chinese)
- [3] Zhao X, Yang C. Analysis and countermeasures of forage seed production in China. *Agricultural Outlook*, 2020; 16(3): 56–61. (in Chinese)
- [4] Li G L. Probe into the application prospect of the advanced technique and equipment for harvesting and processing herbage seed. *Pratacultural Science*, 1999; 6: 3–5. (in Chinese)
- [5] Li B, Sun Q Z, Li F Y. Studies on harvesting methods for seed production of four perennial forage grasses species. *Journal of Anhui Agricultural Sciences*, 2008; 16: 6722–6724. (in Chinese)
- [6] Li B F. *Agricultural mechanics*. Beijing: China Agriculture Press, 2003. (in Chinese)
- [7] Chen M, Jin C Q, Ni Y L, Yang T X, Zhang G Y. Online field performance evaluation system of a grain combine harvester. *Computers and Electronics in Agriculture*, 2022; 198: 107047.
- [8] Wen L, Yao Y M, Yang Y. Constitution analysis of invention patent technology for combine harvester in China. *Chinese Agricultural*

- Mechanization, 2017; 38(3): 131–136.
- [9] Zhang K P, Fan H P, Sun B G, Chai Q. The CFD-DEM gas-solid coupling simulation and experimental verification of cleaning device of wheat combine harvester for intercropping system. *Agricultural Research in the Arid Areas*, 2019; 37(1): 268–274. (in Chinese)
- [10] Ma L C, Wei L B, Pei X Y, Zhu X S, Xu D R. CFD-DEM simulations of particle separation characteristic in centrifugal compounding force field. *Powder Technology*, 2019; 343: 11–18.
- [11] Dai F, Song X F, Guo W J, Zhao W Y, Zhang F W, Zhang S L. Simulation and test on separating cleaning process of flax threshing material based on gas–solid coupling theory. *Int J Agric & Biol Eng*, 2020; 13(1): 73–81.
- [12] Feng X, Gong Z P, Wang L J, Yu Y T, Liu T H, Song L L. Behavior of maize particle penetrating a sieve hole based on the particle centroid in an air-screen cleaning unit. *Power Technonology*, 2021; 385: 501–516.
- [13] Li H C, Li, Y M, Gao F, Zhao Z, Xu, L Z. CFD-DEM simulation of material motion in air-and-screen cleaning device. *Computers & Electronics in Agriculture*. 2012; 111–119.
- [14] Gao Y P, Song L L, Wang L J, Wang H S, Li Y H. Behavior of maize grains on the three-dimensional translational vibrating sieve. *Powder Technology*. 2022; 117999.
- [15] Ding B H, Liang Z W, Qi Y Q, Ye Z K, Zhou J H. Improving cleaning performance of rice combine harvesters by DEM-CFD coupling technology. *Agriculture*, 2022; 12(9): 1–19.
- [16] da Silva R C, Cordeiro Júnior J J F, Pandorfi, H, Vigoderis, R B, Guiselini C. Simulation of Ventilation systems in a protected environment using computational fluid dynamics. *Engenharia Agrícola*, 2017; 37(3): 414–425.
- [17] Hu G M. Analysis and simulation of granular system by discrete element method using EDEM. Wuhan. Wuhan University of Technology Press, 2010. (in Chinese)
- [18] Yu A B, Wright B, Zhou Z Y, Zhu H P, Zulli P. Discrete particle simulation of gas–solids flow in a blast-furnace. *Computers & Chemical Engineering*, 2008; 32: 1760–1772.
- [19] Finnemore E J, Franzini J B. *Fluid mechanics with engineering applications*. McGraw-Hill, 2002.
- [20] Zhu P F. Simulation research on grain air-and-screen cleaning process and optimization of key parameters. Hangzhou, China: Zhejiang University, 2019.
- [21] Casarsa L, Giannattasio P. Experimental study of the three-dimensional flow field in cross-flow fans. *Experimental Thermal and Fluid Science*, 2011; 35(6): 948–959.
- [22] Li H C, Li Y M, Tang Z, Xu L Z. Numerical simulation of material motion on vibrating screen of air-and- screen cleaning device based on CFD-DEM. *Transactions of the CSAM*, 2012; 43(2): 79–84. (in Chinese)
- [23] Li J. Research of three-dimensional parallel vibrating screen for grain cleaning. Zhenjiang, People’s Republic of China: Jiangsu University, 2013. (in Chinese)
- [24] Yu W J, Wu R M, Li H. The numerical simulation on temperature field inside the radiation de-enzyme machine based on Fluent-EDEM coupling. *Food and Machinery*, 2019; 35(8): 104–109, 12. (in Chinese)
- [25] Wang L J, Ma Y, Feng X, Song L L, Chai J. Design and experiment of segmented vibrating screen in cleaning device of maize grain harvester. *Transactions of the CSAM*, 2020; 51(9): 89–100. (in Chinese)
- [26] Ma Z Y, Wan Q H, Chen W X, Bu K, Yang J Z, Du W L. Design and testing of air-and-screen cleaning device for *Leymus chinensis* seed threshing material. *Journal of Chinese Agricultural Mechanization*, 2022; 43(8): 96–105, 127. (in Chinese)